

Synthesis of High-Surface-Area Alumina Aerogels without the Use of Alkoxide Precursors

Theodore F. Baumann,[†] Alexander E. Gash,[†] Sarah C. Chinn,[†] April M. Sawvel,[‡]
Robert S. Maxwell,[†] and Joe H. Satcher, Jr.*[†]

Chemistry and Material Science Directorate and Energy and Environment Directorate,
Lawrence Livermore National Laboratory, P.O. Box 808, L-092, Livermore, California 94551

Received July 23, 2004. Revised Manuscript Received October 25, 2004

Alumina aerogels were prepared through the addition of propylene oxide to aqueous or ethanolic solutions of hydrated aluminum salts, $\text{AlCl}_3 \cdot 6\text{H}_2\text{O}$ or $\text{Al}(\text{NO}_3)_3 \cdot 9\text{H}_2\text{O}$, followed by drying with supercritical CO_2 . This technique affords low-density ($60\text{--}130\text{ kg/m}^3$), high-surface-area ($600\text{--}700\text{ m}^2/\text{g}$) alumina aerogel monoliths without the use of alkoxide precursors. The dried alumina aerogels were characterized using elemental analysis, high-resolution transmission electron microscopy, powder X-ray diffraction, solid-state NMR, acoustic measurements, and nitrogen adsorption/desorption analysis. Powder X-ray diffraction and TEM analysis indicated that the aerogel prepared from hydrated AlCl_3 in water or ethanol possessed microstructures containing highly reticulated networks of pseudoboehmite fibers, $2\text{--}5\text{ nm}$ in diameter and of varying lengths, whereas the aerogels prepared from hydrated $\text{Al}(\text{NO}_3)_3$ in ethanol were amorphous with microstructures comprised of interconnected spherical particles with diameters in the $5\text{--}15\text{ nm}$ range. The difference in microstructure resulted in each type of aerogel displaying distinct physical and mechanical properties. In particular, the alumina aerogels with the weblike microstructure were far more mechanically robust than those with the colloidal network, based on acoustic measurements. Both types of alumina aerogels can be transformed to $\gamma\text{-Al}_2\text{O}_3$ through calcination at $800\text{ }^\circ\text{C}$ without a significant loss in surface area or monolithicity.

Introduction

High-surface-area aluminas are widely used as catalysts and catalyst supports as well as adsorptive material in separation applications.¹ In addition, micro- and nanocrystalline aluminas are also commonly used as precursor materials for Al_2O_3 -based ceramics.² For these applications, one must be able to reliably control composition, porosity, and surface areas of the aluminum oxide materials. Among the synthetic routes that can be used to prepare aluminas, the sol–gel process provides an excellent method for controlling the structural and textural properties of the resultant aluminum oxide. Sol–gel derived aluminas are typically prepared through the catalyzed hydrolysis and condensation of aluminum alkoxide precursors, such as aluminum isopropoxide or aluminum *sec*-butoxide.^{3–28} Although this approach

has been used to prepare a variety of high-surface-area aluminas, including aerogels and xerogels,^{29–39} aluminum

- * To whom correspondence should be addressed. E-mail: satcher1@llnl.gov.
[†] Chemistry and Material Science Directorate.
[‡] Energy and Environment Directorate.
 (1) For a recent review, see: Euzen, P.; Raybaud, P.; Krokidis, X.; Toulhoat, H.; Le Loarer, J. L.; Jolivet, J. P.; Froidefond, C. In *Handbook of Porous Solids*; Schüth, F., Sing, K. S. W., Weitkamp, J., Eds.; Wiley-VCH: Weinheim, 2002; pp 1591–1677.
 (2) Hudson, L. K.; Misra, C.; Wefers, K. In *Industrial Inorganic Chemicals and Products*; Wiley-VCH: Weinheim, 1999; Vol. 1, pp 26–83.
 (3) Yoldas, B. E. *J. Appl. Chem. Biotechnol.* **1973**, *23*, 803.
 (4) Yoldas, B. E. *J. Mater. Sci.* **1975**, *10*, 1856.
 (5) Yoldas, B. E. *Am. Ceram. Soc. Bull.* **1975**, *54*, 286.
 (6) Yoldas, B. E. *Am. Ceram. Soc. Bull.* **1975**, *54*, 289.
 (7) Chane-Ching, J.-Y.; Klein, L. C. *J. Am. Ceram. Soc.* **1988**, *71*, 83.
 (8) Chane-Ching, J.-Y.; Klein, L. C. *J. Am. Ceram. Soc.* **1988**, *71*, 86.
 (9) Assih, T.; Ayral, A.; Abenoza, M.; Phalippou, J. *J. Mater. Sci.* **1988**, *23*, 3326.
 (10) Oh, C.-S.; Tomandl, G.; Lee, M.-H.; Choi, S.-C. *J. Mater. Sci.* **1996**, *31*, 5321.

- (11) Janosovits, U.; Ziegler, G.; Scharf, U.; Wokaun, A. *J. Non-Cryst. Solids* **1997**, *210*, 1.
 (12) Babonneau, F.; Courty, L.; Livage, J. *J. Non-Cryst. Solids* **1990**, *121*, 153.
 (13) Nass, R.; Schmidt, H. *J. Non-Cryst. Solids* **1990**, *121*, 329.
 (14) Elaloui, E.; Pierre, A. C.; Pajonk, G. M. *J. Catal.* **1997**, *166*, 340.
 (15) Tadanaga, K.; Ito, S.; Minami, T.; Tohge, N. *J. Non-Cryst. Solids* **1996**, *201*, 231.
 (16) Ayral, A.; Phalippou, J.; Droguet, J. C. *Better Ceramics through Chemistry III*; Materials Research Society Symposium Proceedings Vol.121; Materials Research Society: Pittsburgh, PA, 1988; p 239.
 (17) Rezgui, S.; Gates, B. C. *Chem. Mater.* **1994**, *6*, 2386.
 (18) Rezgui, S.; Gates, B. C.; Burkett, S. L.; Davis, M. E. *Chem. Mater.* **1994**, *6*, 2390.
 (19) Vaudry, F.; Khodabandeh, S.; Davis, M. E. *Chem. Mater.* **1996**, *8*, 1451.
 (20) Kurokawa, Y.; Shirakawa, T.; Saito, S.; Yui, N. *J. Mater. Sci. Lett.* **1986**, *5*, 1070.
 (21) Ray, J.; Chatterjee, M.; Ganguli, D. *J. Mater. Sci. Lett.* **1993**, *12*, 1755.
 (22) Ramanathan, S.; Roy, S. K.; Bhat, R.; Upadhyaya, D. D.; Biswas, A. R. *J. Alloys Compd.* **1996**, *243*, 39.
 (23) Ji, L.; Lin, J.; Tan, K. L.; Zeng, H. C. *Chem. Mater.* **2000**, *12*, 931.
 (24) Hernandez, C.; Pierre, A. C. *Langmuir* **2000**, *16*, 530.
 (25) Carnes, C. L.; Kapoor, P. N.; Klabunde, K. J.; Bonevich, J. *Chem. Mater.* **2002**, *14*, 2922.
 (26) Sanchez-Valente, J.; Bokhimi, X.; Hernandez, F. *Langmuir* **2003**, *19*, 3583.
 (27) Liu, S.; Fookan, U.; Burba, C. M.; Eastman, M. A.; Wehmschulte, R. *J. Chem. Mater.* **2003**, *15*, 2803.
 (28) Wilcox, L.; Burnside, G.; Kiranga, B.; Shekhawat, R.; Mazumder, M. K.; Hawk, R. M.; Lindquist, D. A.; Burton, S. D. *Chem. Mater.* **2003**, *15*, 51.
 (29) Mizushima, Y.; Hori, M. *J. Non-Cryst. Solids* **1994**, *167*, 1.
 (30) Mizushima, Y.; Hori, M. *J. Mater. Res.* **1995**, *10*, 1424.
 (31) Suh, D. J.; Park, T. J.; Kim, J. H.; Kim, K. L. *Chem. Mater.* **1997**, *9*, 11904.
 (32) Janosovits, U.; Ziegler, G.; Scharf, U.; Wokaun, A. *J. Non-Cryst. Solids* **1997**, *210*, 1.

alkoxides are very reactive and thus reactions involving these precursors typically require complex solvent mixtures or the addition of chelating agents to control the hydrolysis and condensation rates. Therefore, it would be desirable to develop a sol–gel method that utilizes simple aluminum salts in the preparation of high-surface-area aluminas, avoiding the use of highly reactive alkoxide precursors. Such an advance would present a simple and cost-effective method for the design of new alumina materials for catalysis, separations, and ceramics.

We have recently developed a new sol–gel technique for the synthesis of transition and main-group metal oxide aerogels, xerogels, and nanocomposites.^{40–45} This new method involves the use of epoxides as gelation initiators in the preparation of sol–gel materials. In this approach, the epoxide acts as an acid scavenger in the sol–gel polymerization reaction, driving the hydrolysis and condensation of the hydrated metal species. The slow and uniform increase in the pH of the solution leads to the formation of hydrolyzed metal species, which link together through ololation and oxolation to give a sol of metal oxide particles that subsequently cross-link to produce a monolithic gel. The epoxide is ultimately consumed in the gelation reaction generating ring-opened byproducts. One of the advantages to this technique is that it utilizes simple metal salts (e.g., metal nitrates or halides) as precursors in the sol–gel reaction, eliminating the need for organometallic precursors such as metal alkoxides. In the work presented here, we report the synthesis of high-surface-area alumina aerogels through the sol–gel polymerization of hydrated aluminum salts, $\text{AlCl}_3 \cdot 6\text{H}_2\text{O}$ or $\text{Al}(\text{NO}_3)_3 \cdot 9\text{H}_2\text{O}$, using propylene oxide as the gelation initiator. This technique affords low-density monolithic alumina aerogels without the use of alkoxide precursors. The textural properties of the alumina aerogels prepared by this method compare favorably with those of conventional alkoxide-derived alumina aerogels. One of the interesting aspects of this work is that the anion of the $\text{Al}(\text{III})$ salt used in the sol–gel reaction appears to have a significant impact on the structural and mechanical properties of the aerogel materials.

Experimental Section

Materials and Methods. Aluminum(III) salts, $\text{AlCl}_3 \cdot 6\text{H}_2\text{O}$ and $\text{Al}(\text{NO}_3)_3 \cdot 9\text{H}_2\text{O}$, propylene oxide (Aldrich, 99%) and ethanol (200

proof, Aaper) were all used as received. All syntheses were performed under ambient conditions. In a typical synthesis, $\text{AlCl}_3 \cdot 6\text{H}_2\text{O}$ (2.96 g, 12.3 mmol) was dissolved in 20 mL of a 50/50 v/v mixture of water and ethanol. Propylene oxide (7.86 g, 135 mmol) was then added to the clear solution. The reaction mixture was stirred for 10 min, transferred to plastic molds, and the solutions were allowed to gel at RT for 24 h. Gel formation typically occurred within 2 h, affording transparent monoliths. The gel parts were then soaked in a bath of absolute ethanol for 1 day to exchange the water and reaction byproducts from the pores of the material. The wet alumina gels were processed in a Polaron critical point extractor. The ethanol in the pores of the wet gels was exchanged with liquid CO_2 for 3–4 days, after which the temperature was ramped up to $\sim 45^\circ\text{C}$ while maintaining a pressure of ~ 100 bar. The autoclave was then depressurized at a rate of ~ 7 bar/h, affording the aerogels as transparent monoliths. This particular formulation will be denoted as Al–CWE. To help determine the role of the anion and solvent in gel formation for this system, alumina gels were also prepared from different salts and solvent systems using a procedure similar to the one described above. For example, propylene oxide (7.86, 135 mmol) was added to solutions of (1) $\text{Al}(\text{NO}_3)_3 \cdot 9\text{H}_2\text{O}$ (4.6 g, 12.3 mmol) in absolute ethanol (20 mL), denoted as Al–NE; (2) $\text{AlCl}_3 \cdot 6\text{H}_2\text{O}$ (2.96 g, 12.3 mmol) in water (20 mL), denoted as Al–CW; and (3) $\text{AlCl}_3 \cdot 6\text{H}_2\text{O}$ (2.96 g, 12.3 mmol) in absolute ethanol (20 mL), denoted as Al–CE. The wet gels were processed in a fashion identical to that for Al–CWE, affording the aerogels as transparent or white translucent monoliths. Calcination of the alumina aerogels was performed by heating the aerogel samples to 800°C at $5^\circ\text{C}/\text{min}$ in a furnace and holding at that temperature for 2 h.

Characterization. The bulk densities of the alumina aerogels were determined by measuring the dimensions and mass of the monolithic sample. Elemental analyses were performed by Galbraith Laboratories, Knoxville, TN. Surface area determination and pore volume and size analysis were performed by Brunauer–Emmett–Teller (BET) and Barrett–Joyner–Halenda (BJH) methods using an ASAP 2000 surface area analyzer (Micromeritics Instrument Corporation).⁴⁶ Samples of approximately 0.1 g were heated to 150°C under vacuum (10^{-5} Torr) for at least 24 h to remove all adsorbed species. Nitrogen adsorption data were then taken at five relative pressures from 0.05 to 0.20 at 77 K to calculate the surface area by BET theory. For BJH analyses, average pore size and pore volume were calculated using data points from the desorption branch of the isotherm. High-resolution transmission electron microscopy (HRTEM) was performed on a Phillips CM300FEG operating at 300 keV using zero loss energy filtering with a Gatan energy image filter (GIF) to remove inelastic scattering. The images were taken under bright field (BF) conditions and slightly defocused to increase contrast. The images were recorded on a $2\text{ K} \times 2\text{ K}$ CCD camera attached to the GIF. Powder X-ray diffraction data were collected using an APD3720 PEI automatic powder diffractometer with an analyzing crystal, and $\text{Cu K}\alpha$ radiation was used. Solid-state ^{27}Al magic angle spinning (MAS) NMR spectra were collected using a Bruker DRX-500 NMR spectrometer with an operating ^1H frequency of 500.13 MHz and an operating ^{27}Al frequency of 130.31 MHz with a Bruker 4-mm CPMAS probe. The samples were held under magic angle spinning conditions at a spinning speed of 12 kHz. The ^{27}Al spectra were acquired by means of single pulse excitation using pulse widths of $0.65\ \mu\text{s}$ (1/10 the

- (33) Kobayashi, H.; Tadanaga, K.; Minami, T. *J. Mater. Chem.* **1998**, *8*, 1241.
- (34) Younes, M. K.; Ghorbel, A.; Rives, A.; Hubaut, R. *J. Chem. Soc., Faraday Trans.* **1998**, *94*, 455.
- (35) Osaki, T.; Horiuchi, T.; Sugiyama, T.; Suzuki, K.; Mori, T. *J. Non-Cryst. Solids* **1998**, *225*, 111.
- (36) Poco, J. F.; Satcher, J. H.; Hrubesh, L. W. *J. Non-Cryst. Solids* **2001**, *285*, 57.
- (37) Kureti, S.; Weisweiler, W. *J. Non-Cryst. Solids* **2002**, *303*, 253.
- (38) Khaleel, A. A.; Klabunde, K. J. *Chem. Eur. J.* **2002**, *8*, 3991.
- (39) Krompiec, S.; Mrowiec-Bialon, J.; Skutil, K.; Dukowicz, A.; Pajak, L.; Jarzebski, A. B. *J. Non-Cryst. Solids* **2003**, *315*, 297.
- (40) Baumann, T. F.; Gash, A. E.; Fox, G. A.; Satcher, J. H.; Hrubesh, L. W. In *Handbook of Porous Solids*; Schuth, F., Sing, K. S., Weitkamp, J., Eds.; Wiley-VCH: Weinheim, 2002; Vol. 3, p 2014.
- (41) Gash, A. E.; Tillotson, T. M.; Satcher, J. H.; Poco, J. F.; Hrubesh, L. W.; Simpson, R. L. *Chem. Mater.* **2001**, *13*, 999.
- (42) Gash, A. E.; Satcher, J. H.; Simpson, R. L. *Chem. Mater.* **2003**, *15*, 3268.
- (43) Gash, A. E.; Tillotson, T. M.; Satcher, J. H.; Hrubesh, L. W.; Simpson, R. L. *J. Non-Cryst. Solids* **2001**, *285*, 22.

- (44) Reibold, R. A.; Poco, J. F.; Baumann, T. F.; Simpson, R. L.; Satcher, J. H. *J. Non-Cryst. Solids* **2003**, *319*, 241.
- (45) Clapsaddle, B. J.; Gash, A. E.; Satcher, J. H.; Simpson, R. L. *J. Non-Cryst. Solids* **2003**, *331*, 190.
- (46) Gregg, S. J.; Sing, K. S. W. *Adsorption, Surface Area and Porosity*, 2nd ed.; Academic Press: London, 1982.

nonselective $\pi/2$ pulse length of 6.5 μs) and delay times of 1 s. Shifts were referenced to 0.1 M $\text{Al}(\text{NO}_3)_3$ at 0 ppm. The ^{27}Al triple quantum MAS (3QMAS) experiments were run on a Bruker Avance 400 using a Bruker 4-mm CPMAS probe tuned to 104.2 MHz. A standard two-pulse z -filtered pulse sequence was used.⁴⁷ The nonselective 148 kHz $\pi/2$ pulse length was 1.75 μs at the power levels used. The conversion pulse was optimized at 2.5 μs and the reconversion pulse was optimized to 0.8 μs . The z -filter pulse was 20 μs after the reconversion pulse and was set to 50 μs with 30 dB of additional attenuation on the RF power level. Data were acquired and processed using the States method and the data were shear transformed in the indirect dimension according to Massiot et al.⁴⁸ The resonance frequency was set to the frequency of $\text{Al}(\text{H}_2\text{O})_6^{3+}$ (0 ppm). The elastic moduli of the alumina aerogels were calculated using the measured densities and the longitudinal and shear sound velocities, according to the procedures reported by Gross et al.⁴⁹ Sound velocity measurements were made with a Panametrics ultrasonic analyzer model 5052UA with 180-kHz center frequency transducers. Measurements were made on monolithic right circular cylinders of aerogel with flat smooth parallel cylinder faces and lengths between 1 and 2 cm.

Results and Discussion

Synthesis. Our objective was to develop a straightforward method for the preparation of high-surface-area alumina aerogels without the use of aluminum alkoxide precursors. As we have previously shown, main group and transition metal oxide aerogels and xerogels can be prepared directly from metal salts using epoxides as gelation initiators.^{40–45} Mechanistic studies indicate that the epoxide acts as an irreversible proton scavenger that induces hydrolysis and condensation of the hydrated metal cations.⁴¹ Many metal cations tend to act as acids when solvated in water because charge transfer from the coordinated water molecule to the empty orbitals of the metal ion induces a positive partial charge on hydrogen, making the coordinated water more acidic. The epoxide, when introduced to the reaction, consumes the protons from the hydrated metal species, driving the sol–gel polymerization reaction. The protonated epoxide is ultimately consumed during gelation through a ring-opening reaction with a suitable nucleophile. This process is the basis for the preparation of the alumina aerogels presented here. In solution, the $\text{Al}(\text{III})$ ion forms the hexahydrated complex $[\text{Al}(\text{OH}_2)_6]^{3+}$. This complex can act as an acid, generating a series of hydroxylated species, $[\text{Al}(\text{OH})_h(\text{OH}_2)_{6-h}]^{(3-h)+}$, where h can vary from 0 to 4 depending on the pH of the solution. These hydrolyzed cationic complexes can condense through ololation and oxolation reactions to form polynuclear species, which then serve as the building blocks for the condensed phase.^{50,51} A stable alumina gel comprised of nanometer-sized particles can be obtained if the pH of the reaction solution is increased in a slow and uniform fashion.

In the work presented here, alumina aerogels were readily prepared through the addition of propylene oxide to aqueous or ethanolic solutions of hydrated $\text{Al}(\text{III})$ salts followed by supercritical drying of the resultant gel. In the course of this study, we noted that the reaction solvent and the anion of the aluminum salt had a significant impact on the physical properties of the resultant aerogels. For example, gels prepared from an ethanolic solution of either $\text{AlCl}_3 \cdot 6\text{H}_2\text{O}$ or $\text{Al}(\text{NO}_3)_3 \cdot 9\text{H}_2\text{O}$ formed quite rapidly (<30 min) and exhibited significant shrinkage (30–50%) relative to the original size of the mold. As a result, these aerogels, Al–CE and Al–NE, had higher density (100–130 kg/m^3) and tended to be cracked monoliths or even powders. The gels prepared from the nitrate salt, Al–NE, were white and opaque, whereas the Al–CE monoliths, prepared from the chloride salt, were transparent. When gelation was performed in water with $\text{AlCl}_3 \cdot 6\text{H}_2\text{O}$, the transformation occurred much more slowly (14 h) with minimal shrinkage (5–10%). This material, Al–CW, showed negligible cracking and had lower densities ($\sim 50 \text{ kg/m}^3$), but was quite fragile and difficult to handle. The difference in gelation rates between the ethanol and water reactions may be due to the improved nucleophilicity of the $\text{Al}(\text{III})$ anions (Cl^- and NO_3^-) toward the protonated epoxide in ethanol as compared to that in water. The relative nucleophilicity of the anion in the different reaction media would also explain why we were unable to prepare alumina gels from aqueous solutions of $\text{Al}(\text{NO}_3)_3 \cdot 9\text{H}_2\text{O}$, as nitrate is a poor nucleophile in water.⁴¹

One of the limitations associated with aerogel synthesis is that, in general, aerogels are fragile materials that can be easily damaged upon handling. This characteristic limits their utility in areas where processing or application dictates some structural form with moderate strength, such as laser target components.⁵² Therefore, development of methods that afford low-density aerogel monoliths with improved mechanical properties is important for future aerogel application studies. For that reason, we sought to optimize this procedure so that robust alumina aerogel monoliths could be readily prepared. We determined that this could be accomplished through the addition of propylene oxide to a solution of $\text{AlCl}_3 \cdot 6\text{H}_2\text{O}$ dissolved in a 50/50 water/ethanol mixture with subsequent drying under supercritical conditions. The resultant aerogels, Al–CWE, were transparent, exhibited relatively little shrinkage (5–10%), and, despite their low density (60 kg/m^3), were quite robust.

In regard to nomenclature, all of the aerogels obtained from the above reactions are most likely aluminum oxyhydroxides. Elemental analyses of the as-prepared materials did not correlate with the theoretical values for well-crystallized boehmite, $\text{AlO}(\text{OH})$, likely due to the association of additional water within the aluminum oxide structure. Results of the elemental analyses also showed that this process generated aerogels containing minimal amounts of carbon (<2.7%), indicating that most of the solvent, epoxide, and epoxide byproducts are removed during the $\text{CO}_2(\text{l})$ exchange and supercritical drying.

Microstructural Characterization. Transmission electron microscopy was used to evaluate the microstructure of the

(47) Ganapathy, S.; Das, T. K.; Vetrivel, R.; Ray, S. S.; Sen, T.; Sivasanker, S.; Delevoeye, L.; Fernandez, C.; Amoureux, J. P. *J. Am. Chem. Soc.* **1998**, *120*, 4752.

(48) Massiot, D.; Touzo, B.; Trumeau, D.; Coutures, J. P.; Virlet, J.; Flourian, P.; Grandinetti, P. *J. Solid State Magn. Res.* **1996**, *6*, 73.

(49) Gross, J.; Reichenauer, G.; Fricke, J. *J. Phys. D* **1988**, *21*, 1447.

(50) Brinker, C. J.; Scherer, G. W. *Sol–Gel Science*; Academic Press: Boston, MA, 1990; p 59.

(51) Baes, C. F.; Mesmer, R. E. *The Hydrolysis of Cations*; John Wiley & Sons: New York, 1976; p 160.

(52) Hrubesh, L. W. *J. Non-Cryst. Solids* **1998**, *225*, 335.

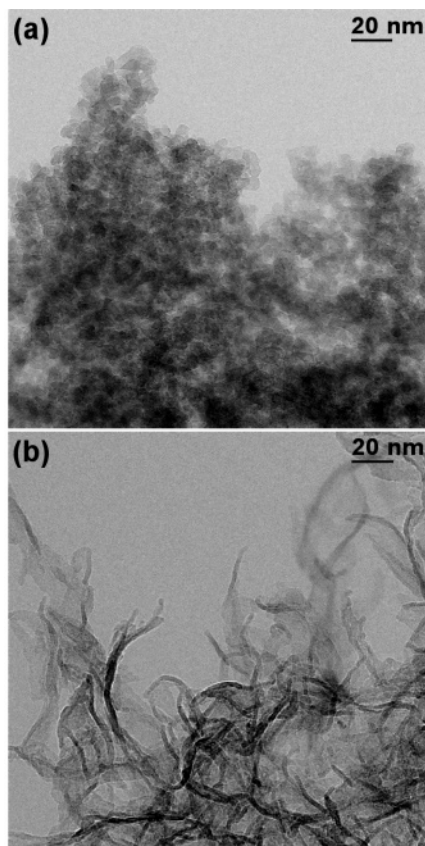


Figure 1. TEM images of alumina aerogels (a) Al-NE prepared from $\text{Al}(\text{NO}_3)_3 \cdot 9\text{H}_2\text{O}$ in EtOH and (b) Al-CWE prepared from $\text{AlCl}_3 \cdot 6\text{H}_2\text{O}$ in $\text{H}_2\text{O}/\text{EtOH}$.

alumina aerogels (Figure 1). The TEM images of the alumina aerogels show that the materials consist of interconnected networks of nanometer-sized particles. Interestingly, however, the aerogels prepared from the chloride salts possess a microstructure much different from those prepared from the nitrate salt. The aerogel Al-NE is comprised of interconnected spherical particles with diameters in the 5–15 nm range (Figure 1a). This type of “colloidal” microstructure is common for many main group and transition metal oxide aerogel materials.⁴⁰ By contrast, the aerogels prepared from the chloride salt in water and/or ethanol (Al-CE, Al-CW, and Al-CWE) consist of fibrous particles, 2–5 nm in diameter and of varying lengths, interconnected to form a weblike microstructure (see representative fibrous structure in Figure 1b). This fibrous morphology is commonly reported for alumina materials prepared from alkoxide precursors.^{25,30,36}

On the basis of these structural differences, it appears that the chloride and nitrate anions have different effects on the formation of the alumina network. Previous work on the sol-gel chemistry of transition metal oxides has shown that anions play both a chemical and a physical role in the homogeneous precipitation of metal oxides.⁵³ Some anions can be strongly coordinated to the metal cations, thus changing the reactivity of the solvated metal species toward hydrolysis and condensation. Once the colloidal particles have formed, the anions can also modify the aggregation

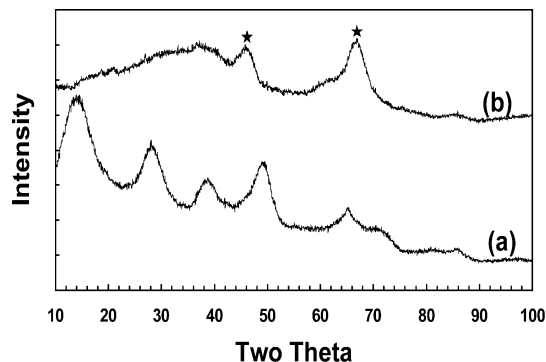


Figure 2. Powder X-ray diffraction patterns for (a) Al-CWE and (b) Al-CWE-800 with the peaks at 46° and 67° marked with an asterisk to denote the [400] and [440] peaks of $\gamma\text{-Al}_2\text{O}_3$.

process through changes to the double layer composition and the ionic strength of the solution. The interaction of the anion with the metal center is, in general, determined by the electronegativity of the anion relative to the ligated water molecules. For the anions used in this study, chloride is typically considered a “noncomplexing” anion and, therefore, one would expect that it would not be involved in formation of the alumina particles. Nitrate, on the other hand, can exhibit “weak-complexing” ability and may be involved in the hydrolysis and condensation reactions. We are currently conducting solution and gel state NMR experiments to probe the extent to which the Al(III) anion influences the formation of the primary alumina particles and the extended aerogel network.

The structural differences observed in these materials are manifested in the mechanical properties of the aerogel monoliths. Monoliths of Al-CWE appeared to be much stiffer and more robust than the other aerogels prepared in this study. Elastic moduli of aerogels can be calculated from sound velocity measurements performed on right circular cylinders of the materials. Using this technique, the elastic modulus of an Al-CWE monolith with a density of 60 kg/m^3 was determined to be 3.2 MPa. The elastic modulus for Al-CWE was higher than those reported for SiO_2 and Al_2O_3 aerogels of similar density.³⁶ For example, an alumina aerogel with a density of 40 kg/m^3 prepared from alkoxide precursors was determined to be 0.55 MPa. Clearly, the highly interconnected weblike microstructure of Al-CWE enhances the mechanical integrity of the low-density aerogel monoliths. Although we wanted to compare this value to that of an aerogel with a “colloidal” microstructure, such as Al-NE, to determine the influence that particle morphology and connectivity has on the mechanical properties of the aerogel, we were unable to prepare monolithic cylinders of that aerogel due to the fragile nature of the Al-NE.

Powder X-ray Diffraction. The aerogels prepared from both the chloride and nitrate salts were characterized using PXRD. The powder X-ray diffraction pattern for Al-NE showed no discernible peaks corresponding to crystalline phases of either aluminum oxyhydroxide, $\text{AlO}(\text{OH})$, or aluminum hydroxide, $\text{Al}(\text{OH})_3$, indicating that the material is essentially amorphous. The aerogels prepared from aluminum chloride, Al-CE, Al-CW, and Al-CWE, gave broad diffraction lines that correspond to gelatinous or pseudoboehmite, $\text{AlO}(\text{OH})$ (Figure 2a). Pseudoboehmite is

(53) Livage, J.; Henry, M.; Sanchez, C. *Prog. Solid State Chem.* **1998**, *18*, 259.

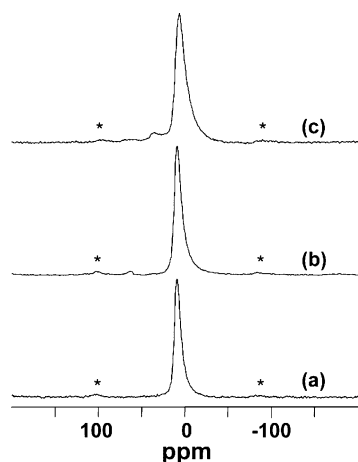


Figure 3. ^{27}Al MAS NMR spectra for (a) Al-CWE, (b) Al-CW, and (c) Al-NE. The smaller peaks marked with asterisks are spinning sidebands of the main peaks.

a poorly crystallized form of boehmite that contains excess water. The lower degree of crystallinity in pseudoboehmite is reflected in broader X-ray diffraction lines. In general, most alumina aerogels or xerogels prepared from alkoxide precursors also exhibit XRD patterns with broad lines corresponding to gelatinous or pseudoboehmite.

The degree of crystalline order in gelatinous aluminas depends critically on the type and concentration of the hydrolyzed Al(III) polycations present during formation of the condensed phase. The nature of these transient Al(III) species is, in turn, dictated by a number of synthetic parameters, such as reaction pH, solvent, temperature, and ionic strength of the solution. Once again, for the materials prepared in this study, it appears that the Al(III) anion used in the reaction influences the crystallinity of the final alumina product. The use of the “noncomplexing” chloride anion favors the formation of a gelatinous boehmite phase in either aqueous or ethanolic reaction solutions, whereas the “weakly complexing” nitrate anion affords gels with no long or intermediate range organization. It is interesting to note that gels prepared from the chloride salt are similar in both particle morphology and crystallinity to those prepared from alkoxide precursors. As mentioned earlier, mechanistic studies using solution and gel state NMR experiments should provide insight into the effect that the anion has with the formation of Al(III) polycations. Nevertheless, the XRD and TEM data appear to indicate that the choice of Al(III) anions can be used to control particle morphology and crystallinity in aerogels prepared by epoxide-initiated gelation.

Solid State NMR. To assess the structure of the Al(III) species that comprise the alumina particles, the aerogels were examined using solid state ^{27}Al MAS NMR (Figure 3). Aluminum NMR chemical shifts are directly related to the coordination number of the Al(III) ion.⁵⁴ Chemical shifts for octahedral Al(III) units appear between -10 and 20 ppm, while tetrahedral Al(III) centers exhibit peaks between 50 and 80 ppm. Resonances for five-coordinate Al(III) species, while less common, are typically observed in the range of 25 – 35 ppm with some field dependence from the residual

Table 1. Physical Properties of Alumina Aerogels Prepared Using Propylene Oxide as the Gelation Agent

aerogel	density (kg/m^3)	specific surface area (m^2/g)	average pore diameter (nm)	pore volume (cm^3/g)
Al-NE	135	709	21	4.3
Al-CE	83	662	36	7.1
Al-CW	52	672	27	7.4
Al-CWE	60	701	24	4.5
Al-NE-800	200	289	32	2.6
Al-CWE-800	100	431	22	2.3

second-order quadrupolar shift.^{55,56} The solid-state ^{27}Al NMR spectra for Al-CE and Al-CWE exhibited single broad resonances at ~ 6 ppm (relative to $[\text{Al}(\text{OH}_2)_6]^{3+}$), indicating the presence of only octahedrally coordinated Al(III) species in the alumina particles (Figure 3a). This observation is consistent with previous work on boehmite gels that showed the extended boehmite network is comprised primarily of octahedral Al(III) subunits.²⁸ The ^{27}Al NMR data for Al-CW showed the presence of both four- and six-coordinate Al(III) species in the aerogel network with a broad resonance at 6 ppm as well as a smaller peak at ~ 63 ppm (Figure 3b). The amorphous Al-NE aerogel appears to be comprised of four-, five- and six-coordinate Al(III) species as the ^{27}Al NMR spectrum for Al-NE shows three peaks at 63, 35, and 6 ppm (Figure 3c). As mentioned earlier, the nature of the hydrolyzed Al(III) polycations present during formation of the condensed phase is dictated by a number of synthetic parameters, such as reaction pH, solvent, temperature, and ionic strength of the solution. For the aerogels prepared in this study, the NMR data suggest that both the reaction anion and solvent influence the type of Al(III) units incorporated into the alumina particles. Solution and gel state NMR experiments will be used to determine the type of hydrolyzed Al(III) polycations present in solution during gelation for these alumina materials.

Nitrogen Adsorption/Desorption Analysis. The surface areas, pore volumes, and average pore diameters for the alumina aerogels were measured using nitrogen adsorption/desorption techniques (Table 1). The alumina aerogels prepared in this study all exhibited surface areas over 600 m^2/g with relatively narrow pore size distributions and average pore diameters in the mesoporous region. The surface areas measured for these epoxide-derived aerogels are equal to or greater than those reported for alumina aerogels prepared from alkoxide precursors. Each of the alumina aerogels exhibited type IV adsorption/desorption isotherms with hysteresis loops at higher relative pressures, a feature that is typically associated with capillary condensation within mesopores. Since the shapes of these loops are related to the structure of the pore network,⁵⁷ it is not surprising to note that there are slight differences in hysteresis for these aerogels. Specifically, the aerogel with the “colloidal” microstructure, Al-NE, had an H1 type hysteresis loop,

(54) MacKenzie, K. J. D.; Snith, M. E. *Multinuclear Solid-State NMR of Inorganic Materials*; Pergamon Press: New York, 2002.

(55) Sato, R. K.; McMillan, P. F.; Dennison, P.; Dupree, R. J. *Phys. Chem.* **1991**, 95, 4483.

(56) Farnan, I.; Dupree, R.; Forty, A. J.; Jeong, Y. S.; Thompson, G. E.; Wood, G. C. *Philos. Mag. Lett.* **1989**, 59, 189.

(57) Rouquerol, F.; Rouquerol, J.; Sing, K. *Adsorption by Powders and Porous Solids: Principles, Methodology and Applications*; Academic Press: London, 1999.

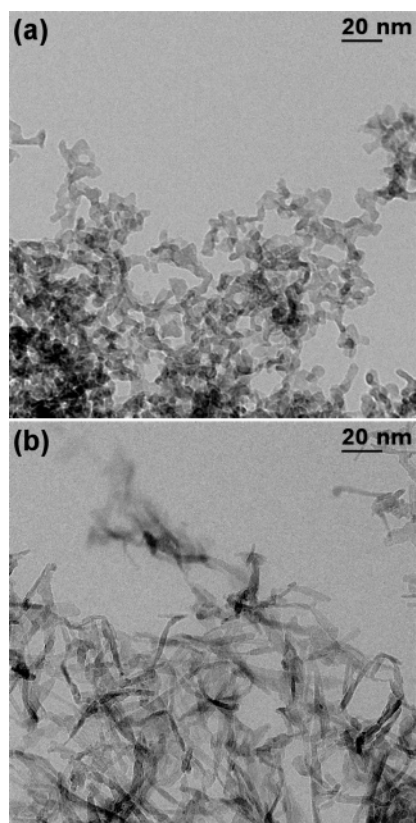


Figure 4. TEM images of calcined aerogels (a) Al-NE-800 and (b) Al-CWE-800.

typically associated with a network structure of spherical primary particles. By contrast, the hysteresis loops for the aerogels with the “weblike” architecture, Al-CE, Al-CW, and Al-CWE, are better characterized as type H3, usually given by adsorbents containing platelike particles or slit-shaped pores. These results are in agreement with those obtained for alkoxide-derived alumina aerogels possessing the fibrous boehmite microstructure.

Heat Treatment. Dehydration of crystalline or fibrillar boehmite through calcination typically affords gamma alumina, γ -Al₂O₃.¹ To determine the effects of dehydration on the alumina aerogels with either the weblike or colloidal microstructure, monoliths of Al-CWE and Al-NE were calcined at 800 °C in air for 2 h. Interestingly, the materials remained monolithic after the heat treatment, but significant shrinkage (~45%) was observed for both types of materials. Not surprisingly, the thermal treatments led to an increase in density and a reduction in specific surface area of the calcined materials relative to the as-prepared aerogels (Table 1). The sintered microstructures of the calcined aerogels were examined by TEM (Figure 4). While the microstructure of Al-CWE-800 retains the fibrous morphology of the as-prepared Al-CWE, the extended network of Al-NE-800 now appears comprised of fused alumina particles, quite different from the as-prepared Al-NE aerogel. Despite these changes, the surface areas of these materials are still reasonably high, with that for Al-CWE-800 exceeding 400 m²/g.

It has been shown previously that the collapse of the boehmite layers during calcination leads to the face-centered cubic close packing of oxygen in γ -Al₂O₃. As a result, the

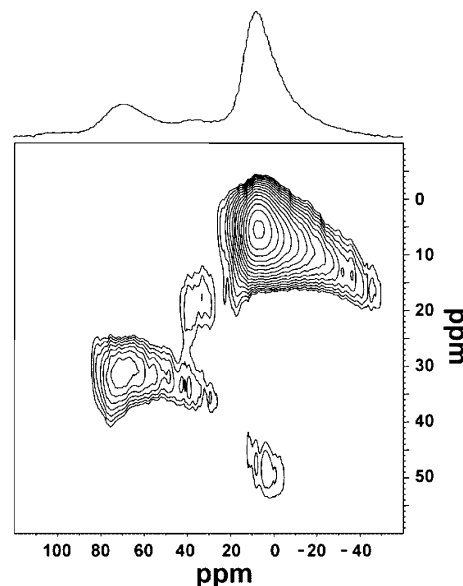


Figure 5. 1D and 2D ²⁷Al 3Q-MAS NMR spectra for Al-NE-800.

intensity of the (400) and (440) lines, the reflections associated with oxygen, tend to dominate the XRD pattern for γ -Al₂O₃. The XRD patterns for both Al-NE-800 and Al-CWE-800 gave broad diffraction lines at 46° and 67° that coincide with the (400) and (440) reflections of γ -Al₂O₃, indicating a phase change within the aerogel structure (Figure 2b). This rearrangement is also confirmed by solid-state ²⁷Al NMR spectroscopy. During the structural transformation of boehmite into γ -Al₂O₃, a portion of the aluminum atoms migrate from octahedral sites to tetrahedral sites in the alumina lattice. The ²⁷Al NMR spectra for the calcined aerogels show a large peak at ~63 ppm, attributable to tetrahedrally coordinated Al(III) atoms in the alumina aerogel matrixes. These results indicate that a phase change can be induced in the as-prepared alumina aerogels without a significant loss in surface area or monolithicity. Surprisingly, the spectrum for Al-NE-800 still displays a peak attributable to five-coordinate Al(III) species (~35 ppm) after calcination (Figure 5). Coordinatively unsaturated Al(III) sites, namely four- and five-coordinate species, serve as the Lewis acid sites of alumina and are of particular interest in catalysis. The presence of the five-coordinate Al(III) species in Al-NE-800 was confirmed by triple quantum-magic angle spinning (3Q-MAS) NMR experiments (Figure 5).

Conclusions

In this report, we describe a straightforward sol-gel method for the preparation of high-surface-area alumina aerogels from simple Al(III) salts using propylene oxide as the gelation initiator. The physical properties of the alumina aerogels prepared by the epoxide-initiated gelation compare favorably with those of aerogels generated from alkoxide precursors. In the course of this study, it was noted that the anion of the Al(III) salt used in the sol-gel reaction had an impact on the architecture of the condensed alumina phase. Aerogels prepared from Al(NO₃)₃ were comprised of amorphous spherical particles and possessed little structural integrity, while monoliths prepared from AlCl₃ were much stronger and contained a weblike microstructure made up

of pseudoboehmite fibers. The ability to control morphology in these materials through the proper selection of anion, as opposed to the addition of chelating agents or complex solvent systems to the sol–gel reaction, would present a simple and cost-effective method for the design of new alumina materials for catalysis, separations, and ceramics.

Acknowledgment. This work was performed under the auspices of the U.S. Department of Energy by Lawrence Livermore National Laboratory under contract W-7405-ENG-48. Special thanks to J. Harper for TEM analysis and C. Saw for X-ray diffraction data.

CM048800M